Geochemical Perspectives Letters



# Aqueous concentration of $CO_2$ in carbon-saturated fluids as a highly sensitive oxybarometer

**F. Miozzi, S. Tumiati**

## Supplementary Information

The Supplementary Information includes:

- $CO_2$-in-fluid Oxybarometer (Excel Spreadsheet)
- S-1 Details on the Evaluation of the Best Fit Model
- S-2 Modelling of Glass-like C Saturated COH Fluids for the Calibration of the Oxybarometer
- S-3 NiO Reagents and Starting Materials
- S-4 Thermodynamic Modelling in Double and Triple Capsule Experiments
- S-5 Parameterisation of the $fO_2$ Dependency from P and T for the Fayalite-Quartz-Magnetite (FMQ) Equilibrium
- Figures S-1 to S-4
- Supplementary Information References

## $CO_2$-in-fluid Oxybarometer (Excel Spreadsheet)

The $CO_2$-in-fluid Excel spreadsheet is available for download from the online version of the article at http://www.geochemicalperspectivesletters.org/article2040.

## S-1 Details on the Evaluation of the Best Fit Model

The program, in order to determine the best fitting model, first generate a list of all the possible equations, defined by the provided variables, and fitting the given data. Within all the possible equations, the best fit solution is the one with the higher quality according to four different statistical criteria. $R^2$ and the Adjusted $R^2$, defining how close the model is to the observed data. In respect to $R^2$, the adjusted $R^2$ is also modified to account for the number of parameters considered in the model. AIC and BIC, respectively the Aikake information criteria and the Bayesian information criteria that are based on the likelihood function and serve to assess the quality of the model. Also these two criteria take in account the number of parameters, as both have a penalisation term if their number is high. While $R^2$ and the Adjusted $R^2$ have a value comprised between 0 and 1, where at 1 the model coincide with

the observed data, the lower is the value for AIC and BIC, higher is the quality of the fit. In the present study the chosen model is the one that minimise the value of the AIC.

## S-2 Modelling of Glass-like C Saturated COH Fluids for the Oxybarometer's Calibration

Modelling the composition of a COH fluid saturated with glass-like C instead of graphite requires the use of different equilibrium constants ($K_p$s) for the reactions involving carbon (see equations (6)-(9) in Tumiati *et al*,. 2020).

The variation of $K_p$s depends on the difference in the Gibbs free energy (*i.e*. ΔG) between graphite and glass-like C. Once the ΔGs for both type of carbon are calculated, it is possible to use the standard $K_p$s and those determined by Tumiati *et al.* (2020) for glass-like C (at 10 Kbar and 800 °C), to establish the constant relating the difference in ΔGs and the difference in $K_p$s. Such constant is the same at all pressure and temperatures, hence, knowing the ΔGs it is possible to use these two parameters to calculate the $K_p$s at all P and T conditions. The Gibbs free energy of formation of both graphite and glass-like C were calculated using the routine "Frendly" in the Perple_X package (Connolly 2005; http://www.perplex.ethz.ch/), with the hp04ver.dat thermodynamic database modified to include glass-like carbon with the preferred model as in Tumiati *et al.*, (2020).

As carbon saturated COH fluids at fixed P, T condition are thermodynamically univariant, the oxygen fugacity is constrained once the composition is known, hence it is possible to determine the $fO_2$ from $XCO_2$ and vice-versa. Accordingly, we used the solver tool on the Gfluid Excel spreadsheet (Zhang and Duan 2009) and providing the $XCO_2$ value retrieved from the experiment, the program iteratively changed the oxygen fugacity until the calculated fluid composition matched the given one. The standard version of the spreadsheet was used for graphite saturated COH fluids. Conversely, for glass-like C saturated fluids, the equilibrium constants of the reactions involving carbon were replaced with those calculated following Tumiati *et al.* (2020).

## S-3 NiO Reagents and Starting Materials for the Experiments

The two commercial nickel oxides were respectively nickel oxide black nanopowder (Sigma-Aldrich Product 72257) and nickel oxide green nanopowder (Sigma-Aldrich. Product 399523-100G). Sintered nickel oxide, was obtained sintering in air a batch of NiO green nanopowder at 1300°C for 72 h. $Ni(OH)_2$ was produced drying at 75°C the product of the basification of a $NiCl_2$ solution with $Na(OH)_2$.
Oxalic acid dihydrate (OAD) which decomposes at T> 200 °C to $CO_2$, $H_2O$ and $H_2$, was used as a fluid source and glass-like C as the carbon reservoir. Their addition to the list of NIST's standards list and thorough thermodynamic characterization from Tumiati and co-authors (2020).

## S-4 Thermodynamic Modelling in Double and Triple Capsule Experiments

In double and triple capsule experiments the buffer reaction with water controls the hydrogen fugacity ($f H_2$) in the outer capsule (eq. 1 in Tumiati *et al.*, 2020). Thanks to the permeability of the inner capsule to $H_2$, the $f H_2$ equilibrium in the inner capsule is reached with $f H_2$-dependent reactions (eq. 4 and 5 in Tumiati *et al.*, 2020) taking place in the GCOH fluid.

Accordingly, using $fH_2$ as a constrain and the proper equations of state (i.e. modelling a $CO_2$-$H_2O$ fluid in the inner capsule and $H_2O$ fluid in the outer capsule), it is possible to retrieve the log $fO_2$ of the fluid in the inner capsule from the buffer's $fO_2$ and vice-versa.

The GFluid Excel spreadsheet and the Zhang and Duan (2009) COH fluid EoS were used for the COH fluids, using the solver obtains $fH_2$ from the $XCO_2$ of the experiments and to determine $XCO_2$ form the $fH_2$ of the NNO reference. For the experiments, once the $fH_2$ is known, the $fO_2$ of the buffering assemblages is obtained by tabulating all the possible values, with the X(O) H-O HSMRK/MRK hybrid-EoS from the "fluids" routine in Perple_X (Connolly 2005; http://www.perplex.ethz.ch/) and finding the one that corresponds to the obtained $fH_2$.
For the NNO reference instead, the $fO_2$ of the buffering assemblage at the desired P-T conditions was calculated with the "vertex" routine in Perple_X and used to determine the corresponding $fH_2$ from the values tabulated with the X(O) H-O HSMRK/MRK hybrid-EoS from the "fluids" routine.

## S-5 Parameterisation of the $fO_2$ Dependency from P and T for the Fayalite-Magnetite-Quartz (FMQ) Oxygen Buffer

Commonly used references for the FMQ buffer (*e.g.*, Ohmoto and Kerrick 1977, O'Neill 1987, Ballhaus *et al.*, 1991) have an average uncertainty on the $fO_2$ calculation of 0.06 log unit. In the present study the uncertainty on the parameterisation of the $fO_2$ for COH fluids is one order of magnitude lower (*i.e.* 0.005 log units). Accordingly, in order to define the $fO_2$ also in term of ΔFMQ, an estimate of $fO_2$ for FMQ with a compatible uncertainty is needed.

We parameterised the $fO_2$ dependency of the FMQ buffer from P and T using the same fitting routine as for the parameterisation of the $CO_2$-in-fluid oxybarometer. The data used for the fit were calculated with the "vertex" routine of the Perple_X package (Connolly 2005). The resulting parametrisation with P in Kbar, T in °C and $XCO_2$ in mol % is:

$$\text{Log } fO_2^{FMQ} = -320.83 + (0.156252/P^2) - (0.20758/P) + (0.111218 \cdot P) - (0.00015537 \cdot P^2) - (82144.7/T^2) + (3876.2/T) + ((21.7 \cdot P)/T) - (0.057 \cdot T) - (0.000051 \cdot P \cdot T) + 50.66 \cdot \log(T) \quad \text{Eq. S-1}$$

The associated uncertainty is in the order of 0.01 log units.

# Supplementary Figures

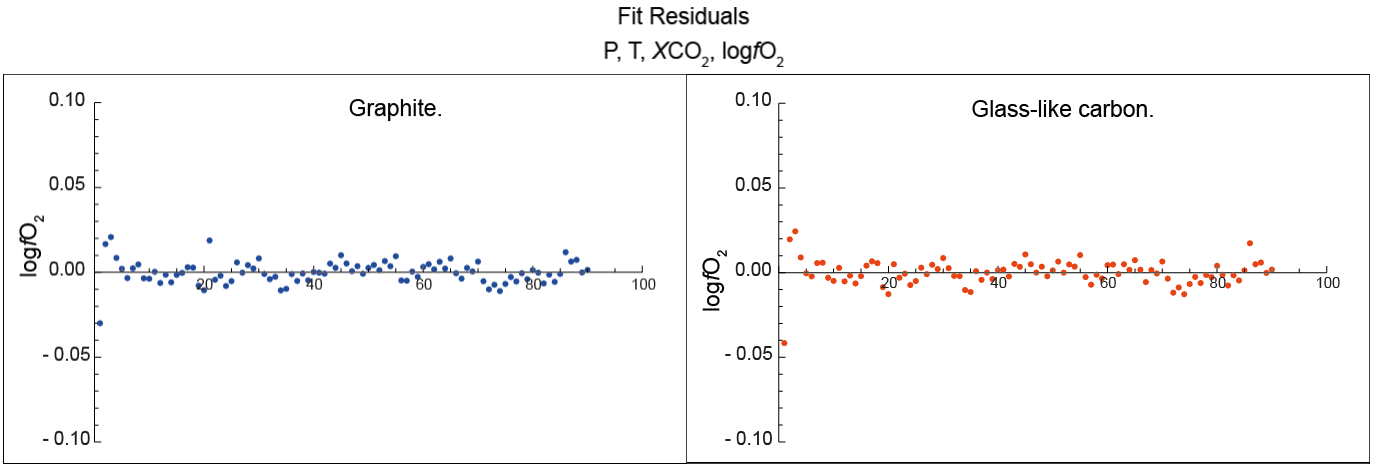


**Figure S-1** Residuals from the fit of COH fluids' data with the chosen polynomial equation. Each point represents the difference between the $fO_2$ value from the experiments and the $fO_2$ calculated with the model. The results obtained for fluids in equilibrium with graphite (on the left) and glass-like C (on the right) are shown.

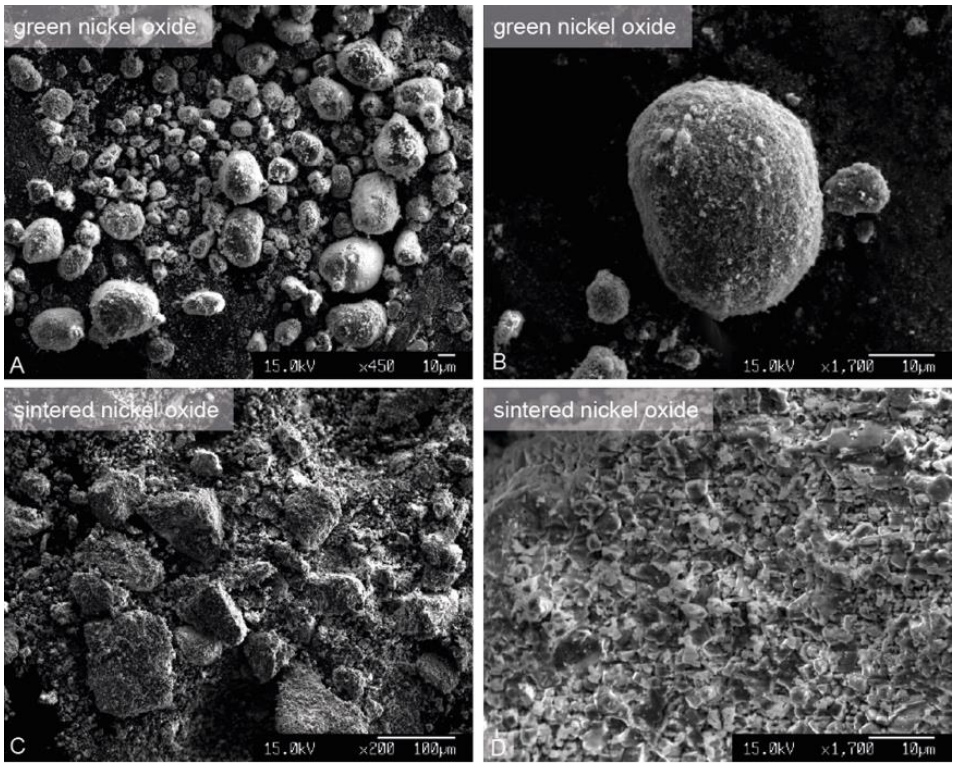


**Figure S-2** Scanning electron microscope images of commercial nickel oxide green nanopowder before and after sintering, taken at 15 KeV. The two different magnifications chosen for each compound offer a better visualisation of the differences in the granulometry and grain distribution.

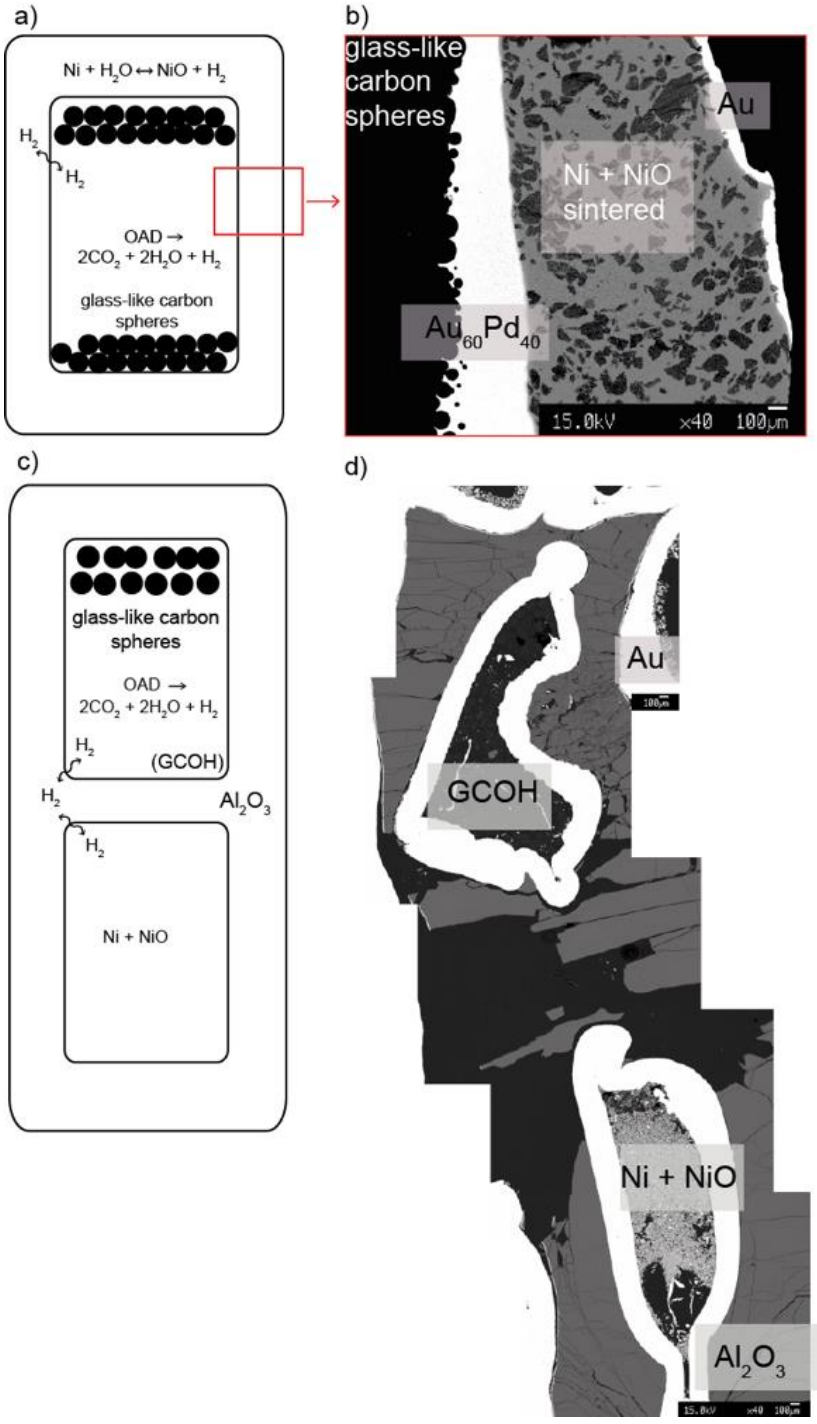


**Figure S-3 Left side**: schemes of the double **(a)** and triple **(c)** capsules used for the experiments. Inner capsule are made in $Au_{60}Pd_{40}$ (OD = 2.3 mm) and the outer in Au (OD = 5 mm).
The inner capsule, permeable to $H_2$ contains oxalic acid dihydrate which decomposes at T> 200 °C to $CO_2$, $H_2O$ and $H_2$, and glass-like carbon. In the double capsule it is embedded in the buffering nickel + nickel oxide (+$H_2O$) assemblage and placed into the outer capsule. In the triple a second inner capsule is filled with the buffering assemblage and both are positioned in the external capsule, embedded in $Al_2O_3$.
**Right side**: backscattered electron images of a double **(b)** and triple capsule **(d)** representative portion.

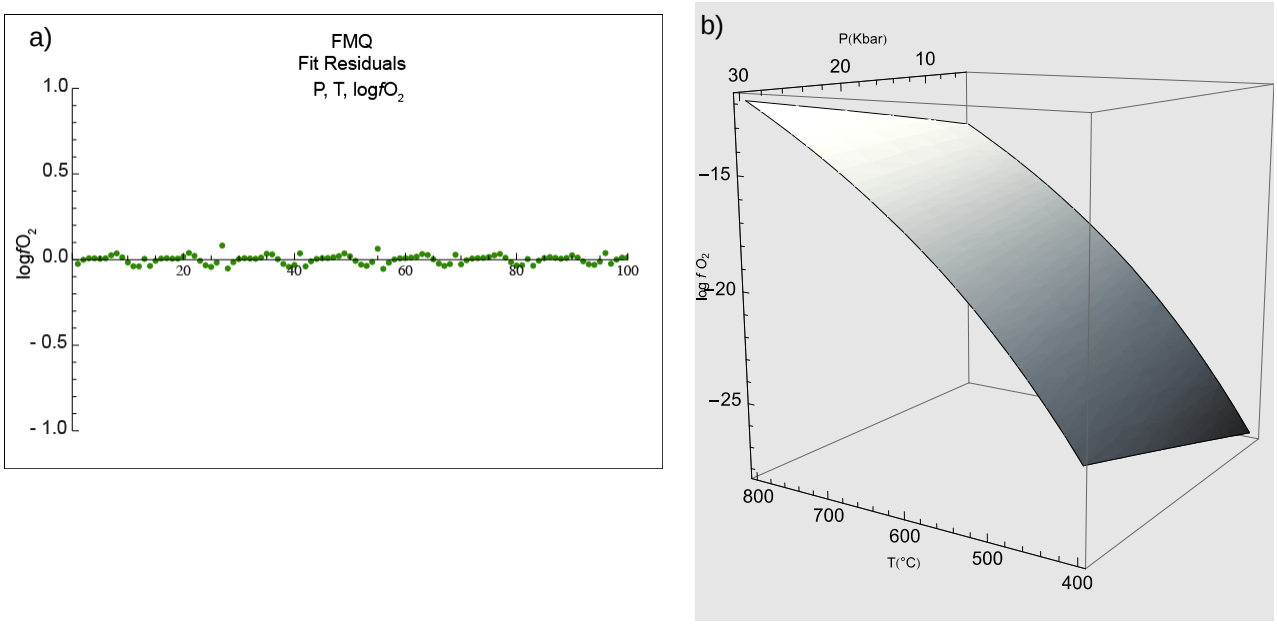


**Figure S-4** Residuals from the fit of the FMQ data **(a)** and representation of the $fO_2$ surface in the P, T, log$fO_2$ space **(b)**.

## Supplementary Information References

Ballhaus, C., Berry, R.F., Green, D.H. (1991) High pressure experimental calibration of the olivine-orthopyroxene-spinel oxygen geobarometer: implications for the oxidation state of the upper mantle. *Contributions to Mineralogy and Petrology* 107, 27-40.

Connolly, J.A. (2005) Computation of phase equilibria by linear programming: a tool for geodynamic modeling and its application to subduction zone decarbonation. *Earth and Planetary Science Letters* 236, 524-541.

Ohmoto, H., Kerrick, D.M. (1977) Devolatilization equilibria in graphitic systems. *American Journal of Science* 277, 1013-1044.

Tumiati, S., Tiraboschi, C., Miozzi, F., Vitale-Brovarone, A., Manning, C.E., Sverjensky, D.A., Milani, S., Poli, S. (2020) Dissolution susceptibility of glass-like carbon versus crystalline graphite in high-pressure aqueous fluids and implications for the behavior of organic matter in subduction zones. *Geochimica et Cosmochimica Acta* 273, 383-402.

Zhang, C., Duan, Z. (2009) A model for C–O–H fluid in the Earth's mantle. *Geochimica et Cosmochimica Acta* 73, 2089-2102.